

Article

Anti-proliferative and migratory inhibition study of b16f10 in mouse melanoma cells induced by synthetic indole-oxadiazole bearing butanamides

Muhammad Athar Abbasi,^{1,2,*} Seong-Hui Eo¹, Aziz-ur-Rehman², Sabahat Zahra Siddiqui², Yohan Han¹, Seon-Mi Yu¹, Song Ja Kim¹, Mubashir Hassan¹, Hussain Raza¹, Syed Anan Ali Shah³ and Sung-Yum Seo^{1,*}

¹ College of Natural Sciences, Department of Biological Sciences, Kongju National University, Gongju, 32588, South Korea.

² Department of Chemistry, Government College University, Lahore-54000, Pakistan.

³ Faculty of Pharmacy and Atta-ur-Rahman Institute for Natural Products Discovery (AuRInS), Level 9, FF3, Universiti Teknologi MARA, Puncak Alam Campus, 42300 Bandar Puncak Alam, Selangor Darul Ehsan, Malaysia.

* Correspondence: abbasi@gcu.edu.pk Tel: +92-42-111000010 Ext. 266.(M.A.A); dnalove@kongju.ac.kr; Tel: +82-416-8508503(S.Y.S)

Received: 25 January 2019; Accepted: 9 February 2019; Published: 30 June 2019.

Abstract: Matrix metalloproteinases-2 and -9 (MMP-2/-9) are key tissue remodeling enzymes that have multiple overlapping activities critical for wound healing and tumor progression. In search of new anti-tumor agents, indole-oxadiazole containing butanamides (1-5) were evaluated with B16F10 mouse melanoma cells in this study. The results showed that compounds 1, 2 and 3 inhibited the cell proliferation in a considerable manner at concentrations ranging from 0-44 μ M. The possible migration inhibitory effects of these melanoma cells were further evaluated through gelatinolytic activity of MMP-2 and MMP-9 secreted from B16F10 cells and it was inferred that compounds 1, 2 and 3 affected the expression and activity of these enzymes in a dose dependent manner while compound 1 can be regarded as promising anti-tumor agent.

Keywords: Indole, oxadiazole, butanamides, anti-proliferation, matrix metalloproteinase, zymography.

1. Introduction

Heterocycles are common structural units in marketed drugs and in medicinal chemistry targets in the drug discovery process. They can serve as useful tools to manipulate lipophilicity, polarity, and hydrogen bonding capacity of molecules, which may lead to improved pharmacological, pharmacokinetic, toxicological, and physicochemical properties of drug candidates and ultimately drugs [1].

The chemistry and pharmacology of indole have been of great interest to medicinal chemists because indole derivatives possessed various biological activities, such as anti-inflammatory [2], antibacterial [3], antimicrobial [4], antifungal [5], antihypertensive [6] and anticonvulsant [7] activities.

The heterocyclic system which contains 1,3,4-oxadiazole nucleus have a rich synthetic history and they are characterized by a wide range of methods of synthesis. 1,3,4-Oxadiazole scaffold, is a vital pharmacophore that displays various pharmaceutical properties [8,9]. Antihypertensive nesapidil, antibiotic furamizole antiretroviral raltegravir, and anticancer agent zibotentan are very few among the marketed drugs that incorporate a 1,3,4-oxadiazole moiety [10].

The significance indole and bisindole-based 1,3,4-oxadiazole heterocycles are also attracting interest due to their wide range of bioactivities, notably as anticancer agents [11,12].

Matrix metalloproteinases (MMPs) are zymogens that are secreted in an inactive pro-form and rapidly proteolytically activated at their site of action. They contain an active site carrying a zinc ion (Zn^{2+}). On the basis of some in vitro assays, these enzymes have been reported to cleave a broad range of extracellular matrix (ECM) molecules, however, the evidences of mice lacking specific MMPs [13-16] and sophisticated mass spectrometry analyses of MMP substrates [17], have exposed that digestion of ECM molecules is not their foremost function in vivo. Instead, several MMPs selectively cleave cytokines, chemokines, cell

surface receptors as well as ECM receptors, and are evolving as decisive fine tuners of cell function in tissue homeostasis and in various pathologies, in particular inflammation [13–15].

There are 23 different human MMPs classified according to their ability to cleave ECM molecules in *in vitro* assays. The best studied MMPs are the gelatinases, MMP-2 and MMP-9, so-called as they can cleave gelatin, the individual alpha chains of denatured collagen type I [16].

Based on their ability to cleave gelatin, several *in vitro* assays have been established that permit detection of MMP-2/ MMP-9 activity in tissue extracts (gelatin gel zymography) or on tissue sections (*in situ* gel zymography). However, distinguishing between these two gelatinases remains difficult, mainly due to the absence of specific antibodies or tools that recognize activated MMP-2 or MMP-9 [14].

Based upon the aforementioned multifarious biological activities of indole and oxadiazole containing molecules, the present study on bi-heterocyclic hybrids was carried out to envisage their anti-proliferative and migratory inhibiting potential of melanoma cells.

2. Experimental

2.1. Synthesis of indole-oxadiazole containing butanamides (1-5)

We have previously reported the synthesis and structural characterization of studied indole-oxadiazole containing butanamides, 1-5 [17]. Those earlier synthesized samples were subjected to current study.

2.2. Cancer cell lines and reagents

The B16F10 melanoma cell line was purchased from KCLB (Korean Cell Line Bank, Seoul, Korea). Penicillin, streptomycin, gelatin, Coomassie blue R-250 and 3-(4,5-Dimethylthiazol-2-yl)-2,5-diphenyltetrazolium bromide (MTT) were obtained from Sigma (St. Louis, MO, USA). Dulbecco's modified Eagle's medium (DMEM) was obtained from Gibco (Grand Island, NY, USA). FBS was from Tissue Culture Biologicals (Long Beach, CA, USA) [18].

2.3. Cell culture

B16F10 cells were cultured in DMEM medium supplemented with 10% *inactivated* FBS, penicillin (50 units/ml) and streptomycin (50 µg/ml), in a humidified atmosphere of 5% CO₂ and 95% air at 37°C. The cells were plated at an appropriate density according to each experimental scale [19].

2.4. Cell viability

The effect of bi-heterocyclic butanamides (1-5) on the viability of B16F10 cells was measured using the MTT assay. Cells were seeded into 96-well plates (0.5×10^5 cells/well in 100 µl medium) and cultured for 24h. The cells were then treated with 1-5 concentration gradient (0, 5.5, 11, 22 or 44 µM) for 24h. After incubation, cells were washed with 1X PBS. Thereafter, the medium was replaced by fresh medium (200 µl) containing 0.5 mg/ml MTT, and the mixture was incubated for 4h at 37°C. After 3h of incubation, the MTT formazan was dissolved in 100 µl solubilization buffer (10% SDS, 0.01 N HCl). The optical absorbance was measured at 570nm by using a microplate reader [19].

2.5. Wound healing assay

Wound healing assay was used to assess cell migration of B16F10 cell lines upon treatments. Briefly, B16F10 cells were seeded 2×10^5 /well cells into 35mm culture dish. After the cells reached 90% confluence, a scratch was made in the cells with a 10 µl pipette tip and washed by 1xPBS and incubated with reagents for 24h. The migration distance of cells was then captured and the images were quantitatively analyzed using ImageJ software (National Institutes of Health, Bethesda, MD, USA). The wound area percentage was calculated as the wound area from 24h vs. the wound area from 0h in each group [18].

2.6. Gelatin zymography analysis

To measure enzymatic activity of MMP-2 and 9 as the key enzymes in the cell invasion and metastasis, gelatin zymography were examined. Briefly, Cells (2×10^5 cells/ml) were seeded in 35mm cell culture dish.

After overnight incubation, B16F10 cells were treated with compounds 1-5 for 24h. At the end of incubation periods, upper medium was centrifuged at 400g for 5 min. Then, 30 μ l of supernatant aliquots of culture medium from each concentration was mixed with 10 μ l of loading buffer 4x (62.5 mM Tris, 4% SDS, 25% glycerol, 0.01% bromophenol blue, PH 6.8). Samples were then loaded on to 7.5% acrylamide gels containing 0.1% gelatin as a substrate and the electrophoresis. After electrophoresis, gels were washed with 2.5% Triton X-100 and then incubated in incubation buffer (10 mM CaCl₂, 150 mM NaCl, and 50 mM Tris-HCl, PH 8.0) for overnight at 37°C. Then gel was stained with 0.5% Coomassie brilliant blue R-250 in 10% acetic acid and 50% methanol [18].

2.7. Statistical analysis

Values are presented as a mean of three different experiments standard deviation (SD). Differences between the calculated means of the each individual group were determined by one-way ANOVA. Any difference was considered statistically significant at $P < 0.05$.

2.8. Computational methodology

2.8.1. Retrieval of matrix metalloproteinase-2 and 9 in Maestro

The MMP-2 and MMP-9 protein structure were retrieved from Protein Data Bank (PDB) (www.rcsb.org) having PDBIDs ICK7 and 1L6J, respectively. The MMP-2 and MMP-9 structures were prepared using the "Protein Preparation Wizard" workflow in Schrödinger Suite. Bond orders were assigned and hydrogen atoms were added to the protein. The water molecules were removed from proteins structures. The structure was then minimized to reach the converged root mean square deviation (RMSD) of 0.30 Å with the OPLS₂₀₀₅ force field. The prepared structures were employed for further grid and docking analysis.

2.8.2. Grid generation and molecular docking

For grid generation preparation, the active site of the enzymes is defined from the co-crystallized ligands from Protein Data Bank and literature data[20–22]. The grid was generated by specify the particular residues which are involve in the active region of target proteins separately for both MMP-2 and MMP-9, respectively. Furthermore, docking experiment was performed against synthesized compound 1 against both receptor molecules separately. The synthesized molecule was sketched by 2D sketcher in Maestro interface. The default docking setup parameters were employed for both ligand-docking experiments [23]. The predicted binding energies (docking scores) and conformational positions of ligands within active region of protein were also performed using Glide experiment. Throughout the docking simulations, both partial flexibility and full flexibility around the active site residues are performed by Glide/SP/XP and induced fit docking (IFD) approaches [24,25]. The 3D and 2D graphical images of both best scored docking complexes were retrieved using Maestro.

3. Results and Discussion

3.1. Chemistry

The synthesis of studied bi-heterocyclic butanamides (1-5) was accomplished in multi-steps according to our reported protocol [17]. The structures of these compounds are shown in Figure 1 and the varying groups in the molecules have been shaded by contours.

3.2. Biological activities

The effects of butanamides (1-5) on cell viability of B16F10 cells were investigated through MTT assay. When B16F10 cells were treated with various concentrations (0, 5.5, 11, 22, and 44 μ M) of studied compounds for 48h, the cell proliferation was reduced significantly by the compounds 1-3, however, the compound 4 and 5 exhibited no remarkable differences in absorbance among the control groups (Figure 2). Cell migration plays important roles in cancer metastasis. Therefore, the migratory effects of these compounds on B16F10 cells were measured. A wound healing migration assay was performed to investigate the inhibition of cell

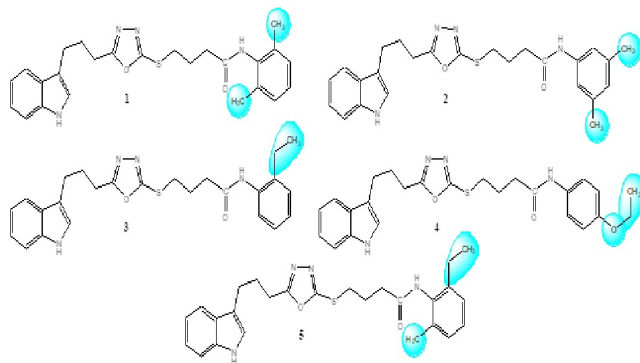


Figure 1. Structures of synthetic indole-oxadiazole bearing butanamides (1-5)

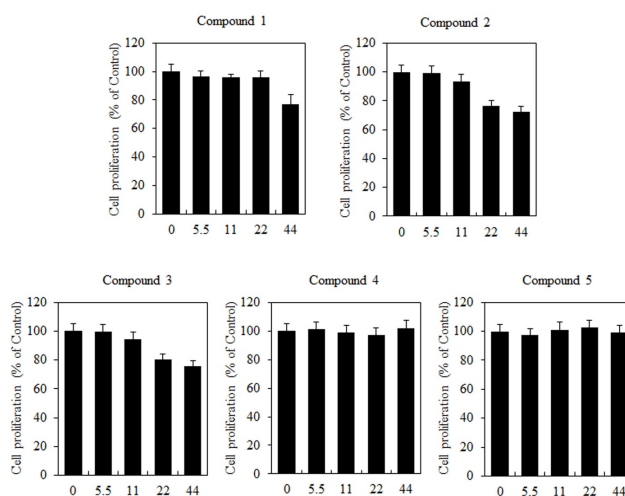


Figure 2. The effects of butanamides (1-5) on cell proliferation of B16F10 cells. Cells were treated with different concentration of these compounds (0, 5.5, 11, 22, and 44 μM) for 48 h. Cell proliferation was measured by the MTT assay. These data are the results of a typical experiment. * $P < 0.05$, compared with untreated cells

mobility. It was observed that cell migration was significantly reduced in B16F10 cells treated with increasing concentrations of compound 1. However, compound 2 and 3 were induced cell migration. The percent of migration was no change in case of 4 and 5, after 48h (Figure 3). Matrix metalloproteinases are important enzymes that degrade extracellular matrix (ECM) components and play important roles in tumor invasion and metastasis. In this regard, the inhibitory effects of butanamides (1-5) were investigated on MMP-2 and MMP-9 enzyme activities through gelatin zymograph assay. From the results, it was rational that MMP-2 and MMP-9 activity was significantly induced by compounds 2 and 3 at 22 - 44 μM concentration in B16F10. These results showed that increase in enzymatic activity in a concentration-dependent manner. However, compared with the control group, compounds 4 and 5 have no effect on said enzymatic activity. Gelatin zymography showed that in case of compound 1, the bands at 72 kDa representing MMP2 activity and 92 kDa showing MMP9 activity were reduced. These results indicated that molecule 1 inhibited proliferation, migration and MMPs, -2 and -9, activity of B16F10 cells (Figure 4).

So, it was hypothesized from our results that compound 1, 2 and 3 inhibited the migration of cells in a dose dependent manner while the compounds 4 and 5 were not effective contributors. However, the peculiar activity of compound 1 might be attributed to the presence of symmetrically di-ortho substituted methyl groups in this molecule.

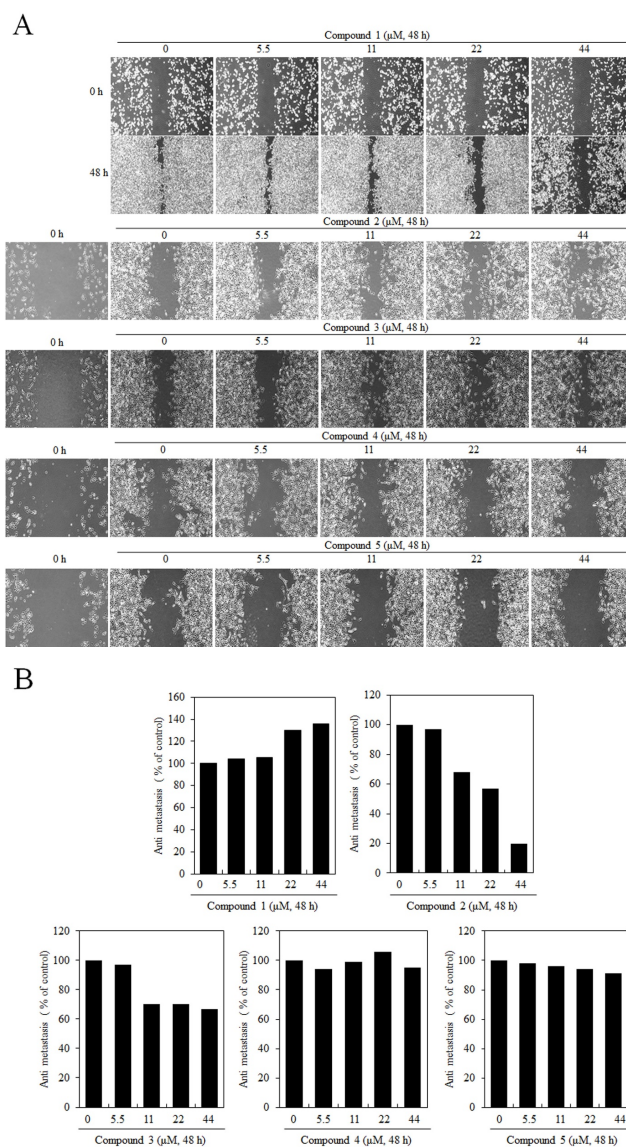


Figure 3. Effects of butanamides (1-5) on B16F10 cell migration. Cells treated with different concentration of these compounds for 48 h. Cell migratory ability was determined by (A) wound-healing assay and (B) migrated cell numbers, were determined by densitometric measurements with ImageJ. The data represented three similar experiments

3.3. Computational analysis

3.3.1. MMP-2 and MMP-9 structural assessment

MMP-2 and MMP-9 are metal containing proteins comprises 631 and 425 residues, respectively. The Ramachandran plots and values showed that both MMP-2 and MMP-9 possessed 92.00 and 92.30% of residues in favored region, respectively. The Ramachandran graph values showed the good accuracy of phi (ϕ) and psi (ψ) angles among the coordinates of receptor and most of residues were plunged in acceptable region. The general structures of both MMP-2 and MMP-9 are mentioned in Figure 5.

3.4. Molecular docking analysis

3.4.1. Glide energy evaluation of synthesized compounds

Molecular docking approach is best approach to study the binding conformation of ligands within the active region of target proteins [25–27]. Based on in vivo results, compound 1 was docked against MMP-2

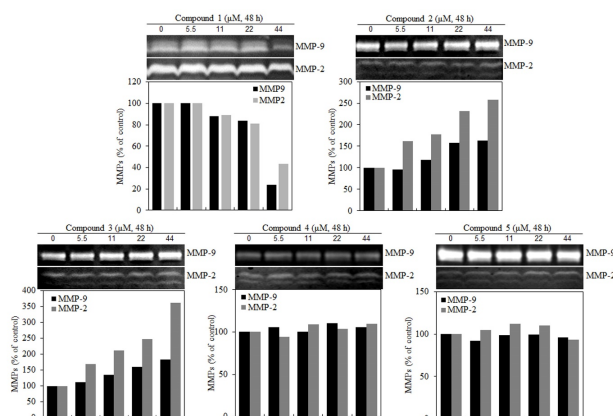


Figure 4. Effect of butanamides (1-5) on B16F10 cell MMP-2, MMP-9 enzymes activity. MMP-2, MMP-9 activity was determined using gelatin zymography and relative activities are quantified densitometrically in ImageJ. These data are the results of a typical experiment. * $P < 0.05$, compared with untreated cells

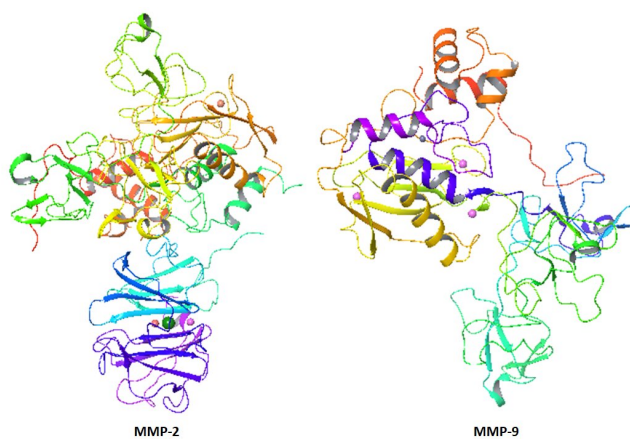


Figure 5. Protein structures MMP-2 and MMP-9

and MMP-9 separately to predict their best conformational position within active site of target proteins. The generated docked complexes of both proteins were examined on the basis of glide docking energy values (kcal/mol) and bonding interaction (hydrogen/hydrophobic) pattern. In MMP-2 and MMP-9 docking results, it has been anticipated that ligand 1 binds within the active region of target proteins with different conformational poses and exhibited good docking energy values -8.90 and -6.663 kcal/mol, respectively.

3.4.2. Ligand-Binding analysis of MMP-2 and MMP-9 docked complexes

The stability of compounds against target proteins depends upon their interactive behavior such as hydrogen and hydrophobic interactions. Figures 6 and 7 showed the binding conformation poses of compound 1 within the active region against target proteins. In MMP-2 docking two hydrogen bonds were at Ile224 and Lys99 with appropriate binding distances. The nitrogen atom of oxadiazolic moiety in compound 1 formed a hydrogen bond with Lys99 possessing bond distance of 2.19 \AA whereas, amidic nitrogen atom showed interaction with Ile424 having bond length 2.55 \AA . In MMP-9 docking results, couple of hydrogen bonds were observed with Glu416 and Arg424 with suitable binding length. Again amidic nitrogen atom of compound 1 interacted through hydrogen bonding with Arg424 having bond length 2.53 \AA whereas, indolic nitrogen atom formed hydrogen bond against Glu416 with bond length 1.63 \AA . The binding distances were in appropriate length and enhance the stability of docking complex stability. Literature data also ensured the importance of these residues in bonding with other MMPs inhibitors which strengthen our docking results [22].

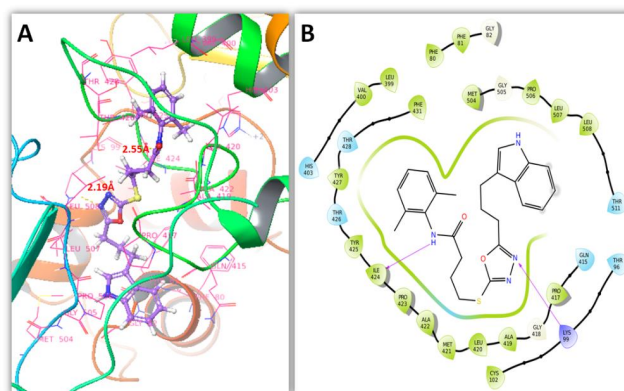


Figure 6. 3D & 2D binding interaction of compound 1 against MMP-2

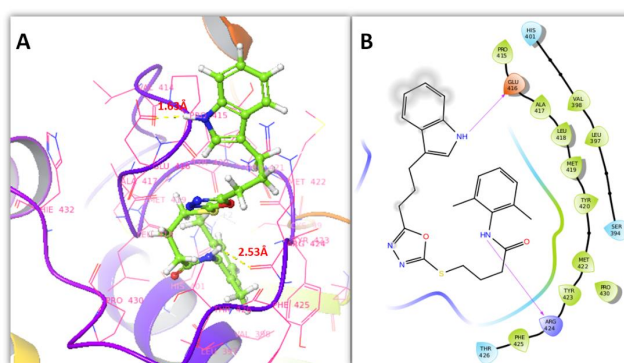


Figure 7. 3D & 2D binding interaction of compound 1 against MMP-9

4. Conclusion

Among the investigated indole-oxadiazole containing butanamides (1-5), the compound 1 exhibited suitable anti-proliferative activity along with possible migratory inhibiting potential for melanoma cells. So, this hybrid molecule might be utilized as conceivable anti-proliferative and antitumor agent in drug designing studies.

Acknowledgments: The present study was supported by Basic Science Research Program through the National Research Foundation of Korea (NRF) funded by the Ministry of Education (2017R1D1A1B03034948).

Author Contributions: All authors contributed equally to the writing of this paper. All authors read and approved the final manuscript.

Conflicts of Interest: "The authors declare no conflict of interest."

References

- [1] Gomtsyan, A. (2012). Heterocycles in drugs and drug discovery. *Chemistry of heterocyclic compounds*, 48(1), 7-10.
- [2] Rani, P., Srivastava, V. K., & Kumar, A. (2004). Synthesis and antiinflammatory activity of heterocyclic indole derivatives. *European journal of medicinal chemistry*, 39(5), 449-452.
- [3] Majik, M. S., Rodrigues, C., Mascarenhas, S., & D'SSouza, L. (2014). Design and synthesis of marine natural product-based 1H-indole-2, 3-dione scaffold as a new antifouling/antibacterial agent against fouling bacteria. *Bioorganic chemistry*, 54, 89-95.
- [4] Sayed, M., Kamal El-Dean, A. M., Ahmed, M., & Hassanien, R. (2018). Synthesis of some heterocyclic compounds derived from indole as antimicrobial agents. *Synthetic Communications*, 48(4), 413-421.
- [5] Xu, H., & Fan, L. I. (2011). Synthesis and antifungal activities of novel indole [1, 2-c]-1, 2, 4-benzotriazine derivatives against phytophthogenic fungi in vitro. *Eur J Med Chem*, 46, 364-369.
- [6] Grasso, S., Molica, C., Monforte, A. M., Monforte, P., Zappala, M., Monforte, M. T., & Trovato, A. (1995). Synthesis and antihypertensive activity evaluation of indole derivatives N-acetamido substituted. *Farmaco (Societa chimica italiana: 1989)*, 50(2), 113-117.

- [7] Srivastava, A., Pandeya, S. N., & Khan, A. A. (2011). Anticonvulsant and Convulsant effects of Indole derivatives against Chemical Models of Epilepsy. *Int. J. Chem. Tech. Res*, 3, 2029-2037.
- [8] Murtuja, S., Shaquiquzzaman, M., & Amir, M. (2018). Design, Synthesis, and screening of hybrid benzothiazolyl-oxadiazoles as anticonvulsant agents. *Letters in Drug Design & Discovery*, 15(4), 398-405.
- [9] Khalilullah, H., J Ahsan, M., Hedaitullah, M., Khan, S., & Ahmed, B. (2012). 1,3,4-oxadiazole: a biologically active scaffold. *Mini reviews in medicinal chemistry*, 12(8), 789-801.
- [10] Guin, S., Rout, S. K., Ghosh, T., Khatun, N., & Patel, B. K. (2012). A one pot synthesis of [1, 3, 4]-oxadiazoles mediated by molecular iodine. *RSC Advances*, 2(8), 3180-3183.
- [11] Sindhe, M. A., Bodke, Y. D., Kenchappa, R., Telkar, S., & Chandrashekar, A. (2016). Synthesis of a series of novel 2, 5-disubstituted-1, 3, 4-oxadiazole derivatives as potential antioxidant and antibacterial agents. *Journal of chemical biology*, 9(3), 79-90.
- [12] Desai, N. C., Somani, H., Trivedi, A., Bhatt, K., Nawale, L., Khedkar, V. M., ... & Sarkar, D. (2016). Synthesis, biological evaluation and molecular docking study of some novel indole and pyridine based 1, 3, 4-oxadiazole derivatives as potential antitubercular agents. *Bioorganic & medicinal chemistry letters*, 26(7), 1776-1783.
- [13] Vandooren, J., Van den Steen, P. E., & Opdenakker, G. (2013). Biochemistry and molecular biology of gelatinase B or matrix metalloproteinase-9 (MMP-9): the next decade. *Critical reviews in biochemistry and molecular biology*, 48(3), 222-272.
- [14] Hannocks, M. J., Zhang, X., Gerwien, H., Chashchina, A., Burmeister, M., Korpos, E., ... & Sorokin, L. (2017). The gelatinases, MMP-2 and MMP-9, as fine tuners of neuroinflammatory processes. *Matrix Biology*.
- [15] Rodríguez, D., Morrison, C. J., & Overall, C. M. (2010). Matrix metalloproteinases: what do they not do? New substrates and biological roles identified by murine models and proteomics. *Biochimica et Biophysica Acta (BBA)-Molecular Cell Research*, 1803(1), 39-54.
- [16] Overall, C. M., & Kleifeld, O. (2006). Validating matrix metalloproteinases as drug targets and anti-targets for cancer therapy. *Nature Reviews Cancer*, 6(3), 227.
- [17] Nazir, M., Abbasi, M. A., Siddiqui, S. Z., Raza, H., Hassan, M., Shah, S. A. A., ... & Seo, S. Y. (2018). Novel indole based hybrid oxadiazole scaffolds with N-(substituted-phenyl) butanamides: synthesis, lineweaver-Üburk plot evaluation and binding analysis of potent urease inhibitors. *RSC Advances*, 8(46), 25920-25931.
- [18] Yu, S. M., & Kim, S. J. (2016). Salinomycin causes migration and invasion of human fibrosarcoma cells by inducing MMP-2 expression via PI3-kinase, ERK-1/2 and p38 kinase pathways. *International journal of oncology*, 48(6), 2686-2692.
- [19] Tavakoli, F., Jahanban-Esfahlan, R., Seidi, K., Jabbari, M., Behzadi, R., Pilehvar-Soltanahmadi, Y., & Zarghami, N. (2018). Effects of nano-encapsulated curcumin-chrysin on telomerase, MMPs and TIMPs gene expression in mouse B16F10 melanoma tumour model. *Artificial cells, nanomedicine, and biotechnology*, 46(sup2), 75-86.
- [20] Elkins, P. A., Ho, Y. S., Smith, W. W., Janson, C. A., D'Alessio, K. J., McQueney, M. S., ... & Romanic, A. M. (2002). Structure of the C-terminally truncated human ProMMP9, a gelatin-binding matrix metalloproteinase. *Acta Crystallographica Section D: Biological Crystallography*, 58(7), 1182-1192.
- [21] Morgunova, E., Tuuttila, A., Bergmann, U., Isupov, M., Lindqvist, Y., Schneider, G., & Tryggvason, K. (1999). Structure of human pro-matrix metalloproteinase-2: activation mechanism revealed. *Science*, 284(5420), 1667-1670.
- [22] Chan-on, W., Huyen, N. T. B., Songtawee, N., Suwanjang, W., Prachayasittikul, S., & Prachayasittikul, V. (2015). Quinoline-based clioquinol and nitroxoline exhibit anticancer activity inducing FoxM1 inhibition in cholangiocarcinoma cells. *Drug design, development and therapy*, 9, 2033.
- [23] Friesner, R. A., Murphy, R. B., Repasky, M. P., Frye, L. L., Greenwood, J. R., Halgren, T. A., ... & Mainz, D. T. (2006). Extra precision glide: Docking and scoring incorporating a model of hydrophobic enclosure for protein-ligand complexes. *Journal of medicinal chemistry*, 49(21), 6177-6196.
- [24] Sherman, W., Day, T., Jacobson, M. P., Friesner, R. A., & Farid, R. (2006). Novel procedure for modeling ligand/receptor induced fit effects. *Journal of medicinal chemistry*, 49(2), 534-553.
- [25] Sherman, W., Beard, H. S., & Farid, R. (2006). Use of an induced fit receptor structure in virtual screening. *Chemical biology & drug design*, 67(1), 83-84.
- [26] Hassan, M., Abbasi, M. A., Siddiqui, S. Z., Hussain, G., Shah, S. A. A., Shahid, M., & Seo, S. Y. (2018). Exploration of synthetic multifunctional amides as new therapeutic agents for Alzheimer's disease through enzyme inhibition, chemoinformatic properties, molecular docking and dynamic simulation insights. *Journal of theoretical biology*, 458, 169-183.
- [27] Hassan, M., Shahzadi, S., Seo, S. Y., Alashwal, H., Zaki, N., & Moustafa, A. A. (2018). Molecular Docking and Dynamic Simulation of AZD3293 and Solanezumab Effects Against BACE1 to Treat Alzheimer's Disease. *Frontiers in computational neuroscience*, 12.



© 2019 by the authors; licensee PSRP, Lahore, Pakistan. This article is an open access article distributed under the terms and conditions of the Creative Commons Attribution (CC-BY) license (<http://creativecommons.org/licenses/by/4.0/>).